Brazilian Journal
of Chemical
Engineering

ISSN 0104-6632
Printed in Brazil
www.abeq.org.br/bjche

Vol. 32, No. 01, pp. 211 - 223, January - March, 2015
dx.doi.org/10.1590/0104-6632.20150321s00003142

DETERMINATION OF THE KINETIC PARAMETERS OF OXY-FUEL COMBUSTION OF COAL WITH A HIGH ASH CONTENT

K. G. P. Nunes* and N. R. Marcílio

[1]Laboratory of Waste Treatment, Department of Chemical Engineering, Federal University of Rio Grande do Sul, (UFRGS), R. Eng. Luiz Englert, s/n, Campus Central, CEP: 90040-040, Porto Alegre - RS, Brazil.
*E-mail: keilagpn@gmail.com, nilson@enq.ufrgs.br

(Submitted: November 28, 2013 ; Revised: April 8, 2014 ; Accepted: May 29, 2014)

Abstract - The aim of this study was to determine the kinetic parameters of the oxy-fuel combustion of *char* from a Brazilian bituminous coal with a high ash content. The *char*, with a particle diameter of 715 μm, was prepared in a N_2 atmosphere at 1173 K. The oxy-fuel combustion assays were performed using a thermobalance at different temperatures and O_2/CO_2 gas mixtures of different concentrations. According to the unreacted core model, the process is determined by chemical reaction at low temperatures, with an activation energy of 56.7 kJ.kmol^{-1}, a reaction order of 0.5 at 973 K and a reaction order of 0.7 overall. The use of the continuous reaction model did not provide a good fit for the experimental data because the consumption of the particles during the reaction was not constant, as predicted by the model. According to the Langmuir-Hinshelwood model, the activation energy for the first step was 37.3 kJ.kmol^{-1}.
Keywords: Char; Oxy-fuel combustion; Thermobalance; Kinetic.

INTRODUCTION

Among the energy sources available worldwide, the most widely used is fossil fuel, especially oil, natural gas and coal, the latter of which represents 28% of the total fossil fuel supply (IEA, 2012). Although 80% of Brazil's domestic energy supply derives from combustion and mineral coal is responsible for 5.2% of the fuels used in combustion, the generation of electrical energy in Brazil is essentially hydroelectric (Ben, 2012). The coal is mainly used in thermoelectric plants (85%), the cement industry (6%), the manufacture of cellulose (4%) and chemical industries (5%) (Soares *et al*., 2008).

The abundance of mineral coal reserves and its geographical distribution, as well as its low cost and stable prices in relation to other fuels, are among the advantages of using this fuel. The greatest disadvantage of the use of this source of fossil energy is the resulting high rate of emission of greenhouse gases. These gases include CO_2, which represent 80% of greenhouse gas emissions (EIA, 2011). Because of great concerns over the levels of CO_2 in the atmosphere, technologies have been developed for its capture and storage (Bachu *et al*., 2007, Buhre *et al*., 2005, Cailly *et al.*, 2005, Middleton *et al*., 2011, Qanbari *et al*., 2011, Toftegaard *et al*., 2010, Stanger and Wall, 2011, Wall *et al*., 2009).

One of the ways to capture CO_2 is oxy-fuel, which consists of burning a carbon source in an O_2 enriched atmosphere, using CO_2 and water as the main combustion gases (Buehre *et al*., 2005, Irfan *et al*., 2011, Middleton *et al*., 2011, Qanbari *et al*., 2011, Stanger and Wall, 2011, Toftegaard *et al*., 2010, Wall *et al*., 2009). Combustion with pure O_2 would lead to a high-temperature flame, therefore CO_2 is recirculated in the burners to control the temperature of the system. The oxy-fuel process comprises simultaneous

*To whom correspondence should be addressed

reactions of combustion and gasification; the main reactions are as follows:

$$C_{(S)} + O_2 \rightarrow CO_{2(g)}$$

$$C_{(S)} + CO_{2(g)} \rightarrow 2\,CO_{(g)}$$

In both processes, coal pyrolysis occurs first, which leads to *char* production. The term 'pyrolysis' describes the devolatilisation of carbonaceous material under a controlled atmosphere and temperature. The volatilised material consists mainly of water vapour, methane and tar, and the solid residue is known as *char*.

Oxy-fuel combustion differs from air combustion in several aspects, including flame temperature (Khatami *et al.*, 2012a), delay in flame ignition (Khatami *et al.*, 2012b) and the reduction of NO_X and SO_X emissions (Kazanc *et al*., 2011); these effects can be explained by the different properties of CO_2 and N_2.

Understanding the behavior of mineral coal in this new combustion environment is important for the adaptation and/or sizing of equipment to yield a clean form of energy production.

Thermogravimetric analysis is widely used as an investigative or comparative tool in the study of thermal events such as combustion and coal pyrolysis.

Several studies conducted in the 1980s addressed the kinetics of coal gasification in Brazil (Schmal *et al*., 1982; José, 1989). For instance, Schmal *et al*. (1982) studied the kinetics of coal gasification between the temperatures of 1073 K and 1273 K with a high-ash coal from southern Brazil. The authors determined that the unreacted core model fit the results up to a temperature of 1123 K and that the continuous reaction model was optimal above this temperature.

Hecht *et al.* (2011) studied a volatile bituminous coal with a high-ash content under different concentrations of O_2 (12, 24 and 36%) at a temperature of 1724 K and observed that the consumption of *char* reached an optimum point in an environment of 24% O_2, where oxidation and gasification accelerate the loss of mass of the particles.

Li *et al.* (2009) pyrolysed a sample of bituminous coal at 1273 K in atmospheres of 100% N_2 and 21%N_2/79%CO_2 using 3 heating rates: 10, 20 and 30 K.min^{-1}. They observed that faster heating of the coal resulted in less time required for pyrolysis, which reduced the loss of mass during devolatilisation and, consequently, increased the proportion of carbonaceous matter. However, little influence of the heating rate was observed during combustion. For oxy-fuel combustion, concentrations of 21, 30, 40 and 80% O_2 in CO_2 were used, and an increase in the concentration of O_2 in the gaseous mixture was observed to reduce the need for high temperatures. The amount of released CO was greater in oxy-fuel combustion, despite the lower levels of SOx and NOx released.

Gil *et al.* (2011) studied four types of *char*: a semi-anthracite, a medium- volatile bituminous and two highly volatile bituminous *chars*, pyrolysed at 1273 K in atmospheres of 100% N_2 and 100% CO_2. The authors concluded that a greater loss of mass occurred during devolatilisation under 100% CO_2 and that the *char* produced exhibited a lower reactivity because of its more stable structure.

Carotenuto *et al*. (2011) studied 3 types of coal under oxy-fuel combustion, including a south Brazilian coal from Mina do Leão II, which is the same coal used in the present study. The temperatures studied were 1073, 1173 and 1273 K in atmospheres of 21% O_2 in CO_2 and 21% O_2 in N_2 (air). The authors reported a greater consumption of O_2 under conditions of oxy-fuel combustion compared to that under conventional combustion. They also observed that an increase in the reaction temperature increased the consumption of O_2.

On the basis of the results of the aforementioned research, experimental parameters were established for this work, including the atmosphere used for pyrolysis, the temperature of the oxy-fuel and the concentration of O_2 in CO_2, to evaluate the kinetic parameters of oxy-fuel combustion. The motivation for this study was based on the need to obtain a permanent set of data to understand the conversion of mineral coal *char* under oxy-fuel combustion conditions. Therefore, the present investigation studied the oxy-fuel combustion of *char* produced in an atmosphere of N_2 from a Brazilian bituminous coal with a high ash content using a thermobalance. The oxy-fuel combustion reaction was studied with concentrations of 10 to 30% O_2 in CO_2 and at temperatures ranging from 973 to 1273 K.

The experimental parameters used to evaluate the kinetics of the oxy-fuel combustion of a Brazilian sub-bituminous coal were selected for the purpose of gathering useful data for the sizing and modelling of fluidised-bed reactors.

MATERIALS AND METHODS

Sample

A sample of *ROM* (run of mine) coal from Mina do Leão II, southern Brazil, which had been crushed

and sieved to yield an average particle diameter of 715 μm was used for the production of *char* in an atmosphere of N_2. The results of the immediate analysis, elemental analysis and surface-area analysis are shown in Table 1:

Table 1: Composition of the coal and the *char* produced.

Analyses	Levels (%)
Proximate analysis	
Volatile analysis[1]	18.4
Ashes[1]	48.7
Fixed carbon[1]	32.9
Elemental analysis[2]	
C	63.4
H	6.4
N	1.6
S	2.1
O	26.5
Surface area[3] - BET ($m^2.g^{-1}$)	29.7

[1]dry basis
[2]ash free dry basis
[3]analysis in the *char* produced.

C*har* Preparation

For the production of *char*, a 0.1 kg sample of coal was placed in a stainless steel reactor (0.14 m high and 0.06 m in diameter), and heated in a muffle furnace, as shown in Figure 1. The unit had an inert gas inlet and an outlet for the gases produced during pyrolysis, as well as a temperature controller and a thermocouple to measure the axial temperature of the reactor. During *char* production, a N_2 atmosphere, a granulometric range of 590 to 840 μm and a temperature of 1173 K were used. The heating rate of the sample was 20 $K.min^{-1}$ from room temperature to the final temperature. After 100 minutes of heating, the sample mass was observed to remain unchanged because all volatile matter had been eliminated. Because of the heterogeneity of the raw material employed, a residence time in the reactor of 105 minutes was established.

Oxy-Fuel Combustion

The oxy-fuel combustion of *char* was analysed with the use of a thermobalance (Netzsch 409) under atmospheric pressure. Approximately 30 mg of *char* was placed in a dish crucible whose base was formed by a platinum screen that allowed the passage of reagent gases through the sample. A thermocouple located below the dish monitored the temperature, which ranged from 973 to 1273 K. The gases used in the experiments were introduced into the thermobalance at a rate of 120 $mL.min^{-1}$, with O_2 concentrations in CO_2 varying from 11 to 30%. The conversion X of *char* was calculated according to Equation (1):

$$X = \frac{M_i - M}{M_i - M_C} \tag{1}$$

where M_i represents the initial mass of the *char* (mg), M is the instantaneous mass (mg), and M_C is the final mass after oxy-fuel combustion (mg) (Levenspiel, 1976).

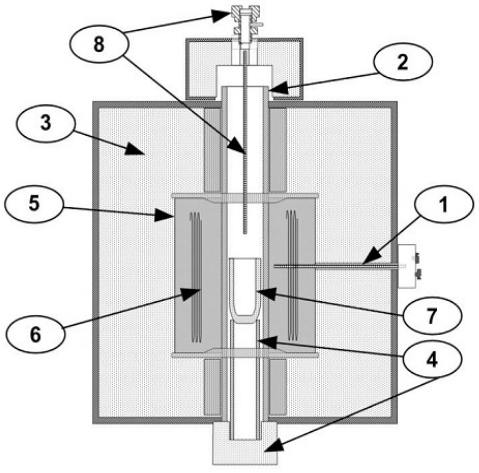

1. Thermocouple
2. Alumina tube
3. Refractory lining
4. Ceramic support for the crucible
5. Heating chamber
6. Resistance heating elements ($MoSi_2$)
7. Reactor
8. Inert gas inlet

Figure 1: Schematic diagram of the furnace used in the experimental study.

Kinetic Model

Models for the interpretation of kinetic data from gas-solid reactions are described in the literature. Three such models were used to model the experimental results obtained and to determine the kinetic parameters of the oxy-fuel combustion reaction of the studied *char*:

Unreacted Core Model: the reaction starts at the outside surface and moves towards the centre of the solid, leaving a layer of inert solid, i.e., ashes. This model considers the occurrence of five sequential steps: 1) diffusion of the reagent gas through the stagnant film of gas at the surface of the solid particle; 2) diffusion of he reagent gas through the ash layer; 3) reaction of the gas with the solid on its surface; 4) diffusion of the gas product generated by chemical reaction through the ash layer; and 5) diffusion of the gas product through the layer of stagnant film of gas around the particle.

Each of the steps is modelled by a mathematical equation based on conversion over time (Barranco *et al*., 2009, Levenspiel, 1976).

Whenever the diffusion of the reagent gas A through the stagnant film of gas on the surface of a solid particle controls the reaction, the reaction can be modelled by Equation (2), where the expression for τ is shown in Equation (3):

$$\frac{t}{\tau} = X \tag{2}$$

$$\tau = \frac{\rho\, R}{3 k_g P_{O_2}} \tag{3}$$

where X is the char conversion, t is the time for the conversion X (s), τ is the time for the full conversion (s), R is the radius of the *char* particles (m), ρ is the specific mass of the *char* sample (kg.m^{-3}), P_{O_2} is the partial pressure of oxygen (kPa) and k_g is the coefficient of mass transfer between the fluid and solid (kg.m^{-2}.s^{-1}.kPa^{-1}).

If the ash layer acts as a barrier controlling the process, then the results can be modelled according to Equation (4), where the expression for τ is shown in Equation (5):

$$\frac{t}{\tau} = 1 - 3(1-X)^{2/3} + 2(1-X) \tag{4}$$

$$\tau = \frac{\rho\, R^2}{6 \mathcal{D}_e P_{O_2}} \tag{5}$$

where X is the char conversion, t is the time for the conversion X (s), τ is the time for the full conversion (s), R is the radius of the *char* particles (m), ρ is the specific mass of the *char* sample (kg.m^{-3}), $\mathcal{D}_e$ is the coefficient of effective diffusivity (m².s^{-1}) and P_{O_2} is the partial pressure of oxygen (kPa).

If the chemical reaction is the limiting step of the reaction, such a gas-solid surface reaction can be modelled according to Equation (6), where the expression for τ is shown in Equation (7):

$$\frac{t}{\tau} = 1 - (1-X)^{1/3} \tag{6}$$

$$\tau = \frac{\rho\, R}{k\, P_{O_2}} \tag{7}$$

where X is the char conversion, t is the time for the conversion X (s), τ is the time for the full conversion (s), R is the radius of the char particles (m), ρ is the specific mass of the *char* sample (kg.m^{-3}), k is the superficial first-order reaction rate constant (kg.m^{-2}.s^{-1}.kPa^{-1}) and P_{O_2} is the partial pressure of oxygen (kPa).

Continuous Reaction Model: the reaction occurs simultaneously across the entire particle as the reagent gas is consumed. This model was developed for cases where the diffusion of the reagent gas is much faster than the chemical reaction involved. Equation (8) represents this model:

$$-\ln(1-X) = kt \tag{8}$$

where X is the char conversion, t is the time for the conversion X (s) and k is the first-order reaction rate constant (s^{-1}).

Langmuir-Hinshelwood Model: this model establishes a formula for the rate of heterogeneous chemical reaction that combines the behaviors of the steps of adsorption, desorption and chemical reaction. The reaction occurs via two elementary steps, (9) and (10):

$$C + O_2 \xrightarrow{k_1} C(O) \tag{9}$$

$$C(O) \xrightarrow{k_2} CO \tag{10}$$

where C(O) represents the species adsorbed on to the particle surface. According to the model, the order of the reaction varies with the oxygen concentration and with temperature, and the model itself should be used for high temperatures. In this case, the reaction rate can be expressed by Equation (11):

$$\left(-r_A\right)=\frac{k_1 k_2 P_{O_2}}{k_1 P_{O_2}+k_2} \tag{11}$$

where ($-r_A$) is the rate of reaction, k_1 (kmol.m^{-2}.s^{-1}) and k_2 (kmol.kPa.m^{-2}.s^{-1}) represent the specific rates of reactions (9) and (10), respectively, and P_{O_2} represents the partial pressure of oxygen (kPa).

Notably, in the Langmuir-Hinshelwood model, the parallel reaction step in the gaseous phase of oxidation of CO (Equation (12)) is not considered.

$$CO+\frac{1}{2}\,O_2 \rightarrow CO_2 \tag{12}$$

RESULTS AND DISCUSSION

Effect of Temperature

To evaluate the effect of temperature on the reaction rate of the oxy-fuel combustion of *char*, the temperatures 973 K, 1073 K, 1173 K and 1273 K were used, and the other variables were fixed. We selected these temperatures on the basis of preliminary results obtained in the thermogravimetric tests shown in Figure 2, which were conducted at Brandenburg University of Technology in Cottbus – Germany using a sample of coal from Mina do Leão II in the granulometric range 0.125 – 0.500 mm (Carotenuto *et al*., 2012).

As shown in Figure 2, the loss of normalized carbon demonstrates consistent behavior up to 1073 K, under both N_2 and CO_2 atmospheres. Above this temperature, the Boudouard reaction occurs, and the carbon is consequently consumed.

Figure 3 shows the curves of *char* conversion as a function of time for the temperatures 973 K, 1073 K, 1173 K and 1273 K with a mixture of 20%O_2/80%CO_2 as the reagent gas.

As evident in Figure 3, an increase in the temperature increases the rate of consumption of *char*, i.e., it increases the reaction rate. At temperatures of 973 K and 1073 K, the behavior of *char* conversion as a function of time is very similar; however, at temperatures of 1173 K and 1273 K, the reaction rate dramatically increases in relation to temperature. Most likely, the increase in temperature causes an increase in the surface area of the *char*, thereby facilitating the access of reagent gases to the sample surface. This behavior indicates that the kinetic regime controls the process.

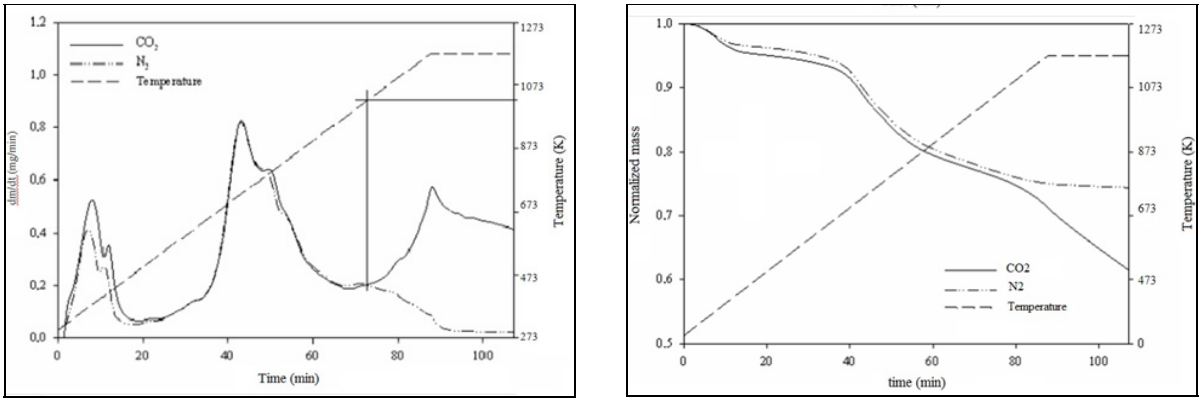

Figure 2: Normalised mass loss and curve of the reaction rate of coal from Mina do Leão II as function of time (granulometry between 0.125 and 0.500 mm). From: Carotenuto *et al*., 2012.

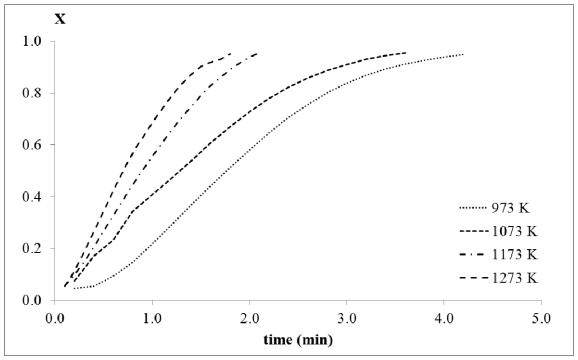

Figure 3: Reaction rate vs. temperature for the mixture 20% O_2/80%CO_2 at 973 K, 1073 K, 1173 K and 1273 K.

Influence of O_2 Concentration in the Gas Mixture

Because of differences in the physicochemical properties of N_2 and CO_2, the ignition of coal is known to be delayed in an oxy-fuel combustion atmosphere when a given concentration of O_2 is added to either N_2 or CO_2. To obtain the same temperature profile as that in atmospheric air, which normally contains 21% O_2 in N_2, a reagent mixture must contain 30% O_2 in CO_2 (Khatami *et al.*, 2012).

Therefore, on the basis of this information, we analysed O_2/CO_2 gas mixtures in the proportions 10% O_2/90% CO_2, 20% O_2/80% CO_2 and 30% O_2/70% CO_2 at temperatures of 973 K, 1073 K, 1173 K and 1273 K, shown in Figures 4 and 5.

At all four temperatures, an increase in the O_2 concentration in the gas mixture increased the rate of conversion of *char*. This phenomenon indicates that the process is determined by chemical reaction, although the overlap of the curves associated with 20% and 30% O_2 in the mixture at a temperature of 1273 K suggest a change in the determining reaction mechanism.

Kinetic Models

Unreacted Core Model

Figures 6 and 7 present the curve fit of the expression for the unreacted core model to the experimental data obtained at 973 K, 1073 K, 1173 K and 1273 K for the model in which the diffusion in the gas layer outside the particle controls the reaction and the diffusion of the reagent gas in the layer of ash, respectively.

As evident in Figures 6 and 7, the models do not adequately reproduce the measurements because a continuous change occurs in the slope of the straight lines, indicating a change of reaction control.

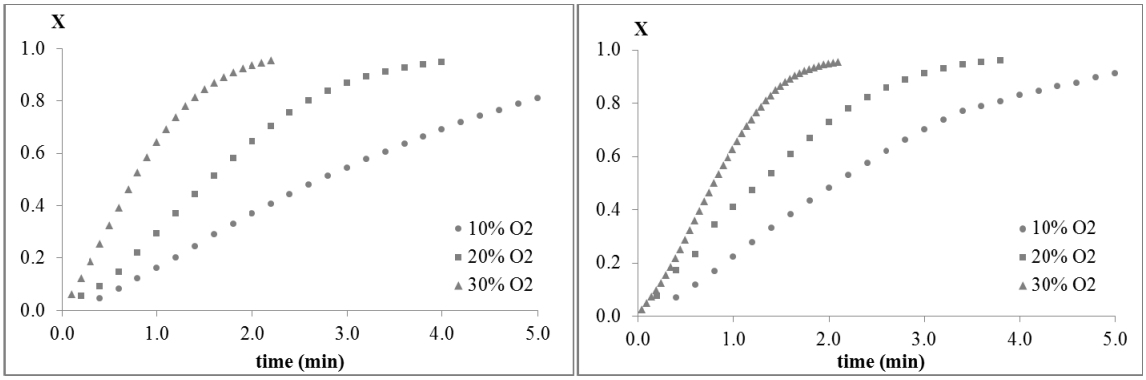

Figure 4: Conversion of *char* vs. time for different concentrations of the O_2/CO_2mixture at 973 K and 1073 K.

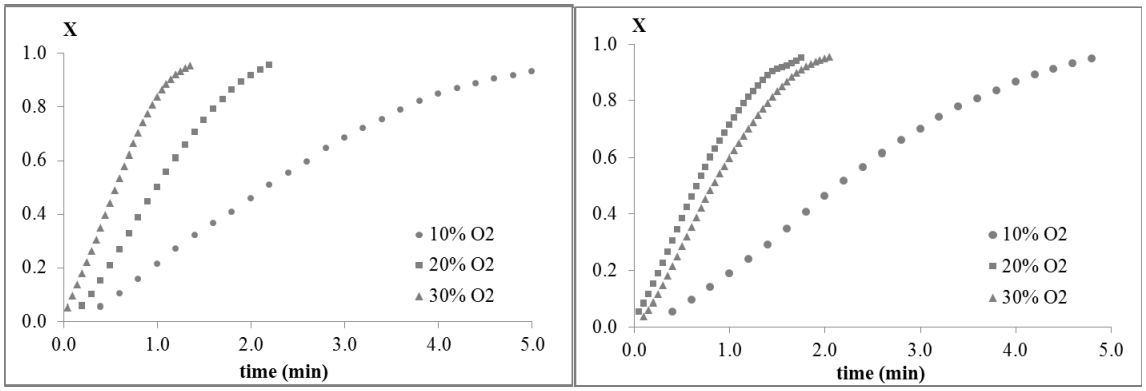

Figure 5: Conversion of *char* vs. time for different concentrations of the O_2/CO_2 mixture at 1173 K and 1273 K.

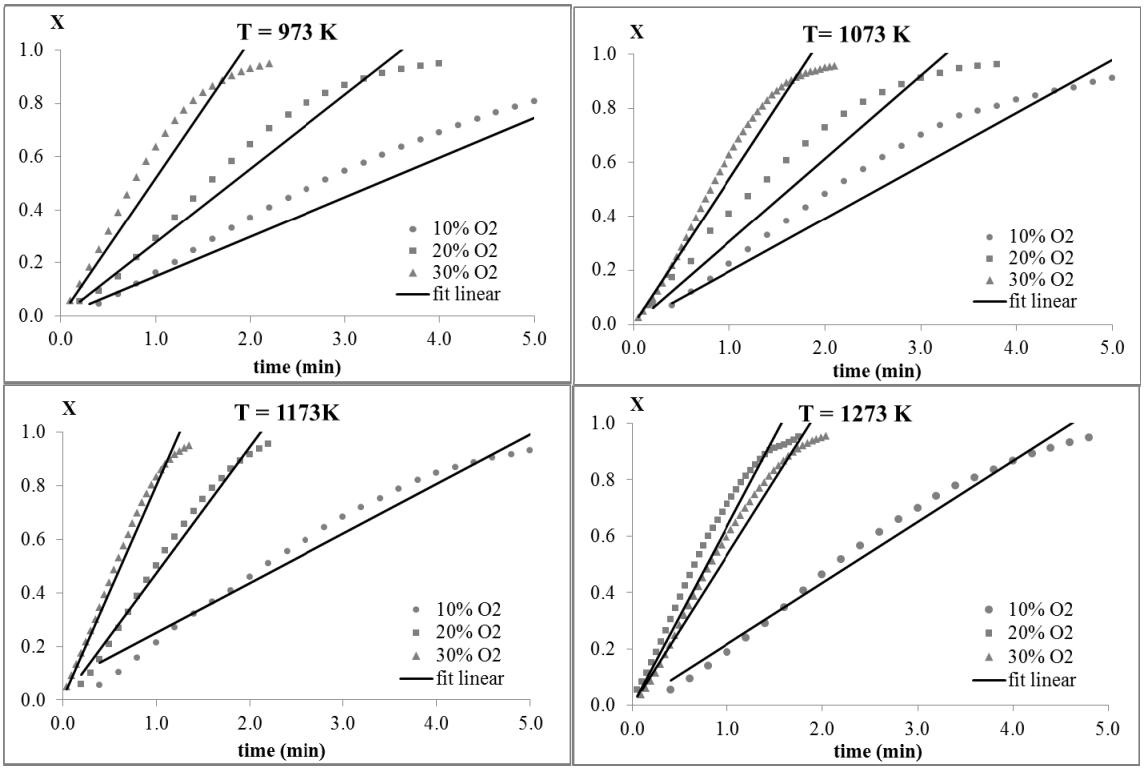

Figure 6: Curve fit of the expression for the unreacted core model when diffusion in the layer outside the particle controls the process and the curves of char conversion as a function of time for the temperatures 973 K, 1073 K, 1173 K and 1273 K.

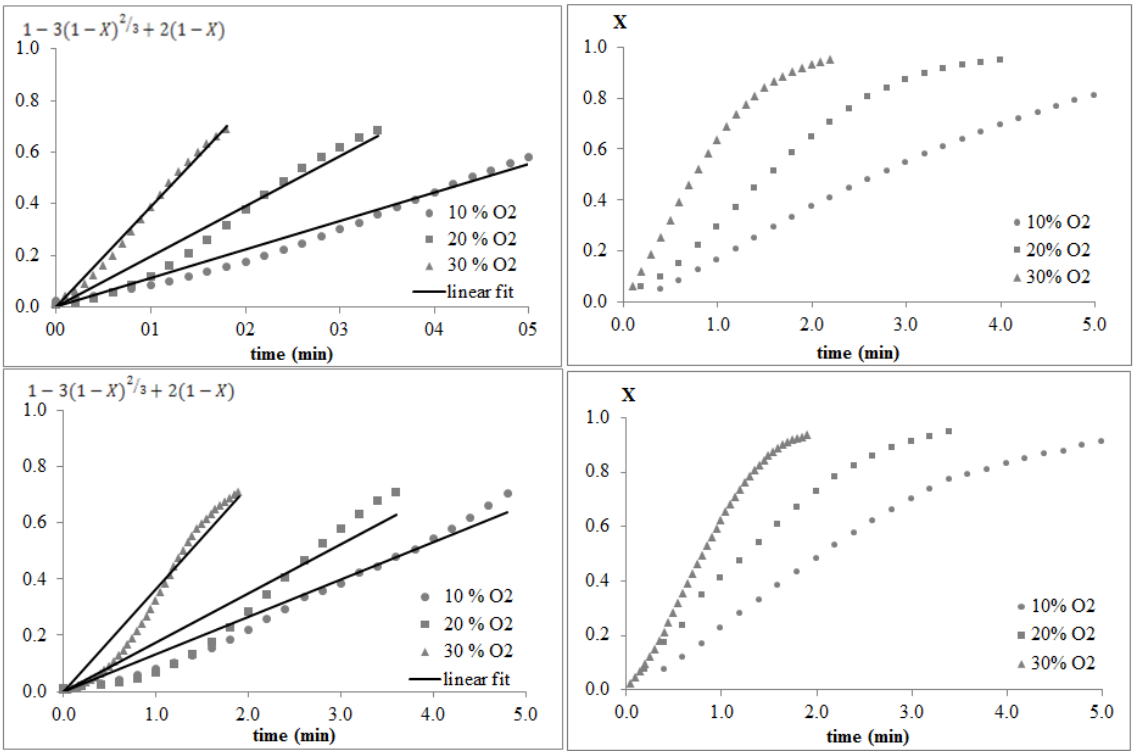

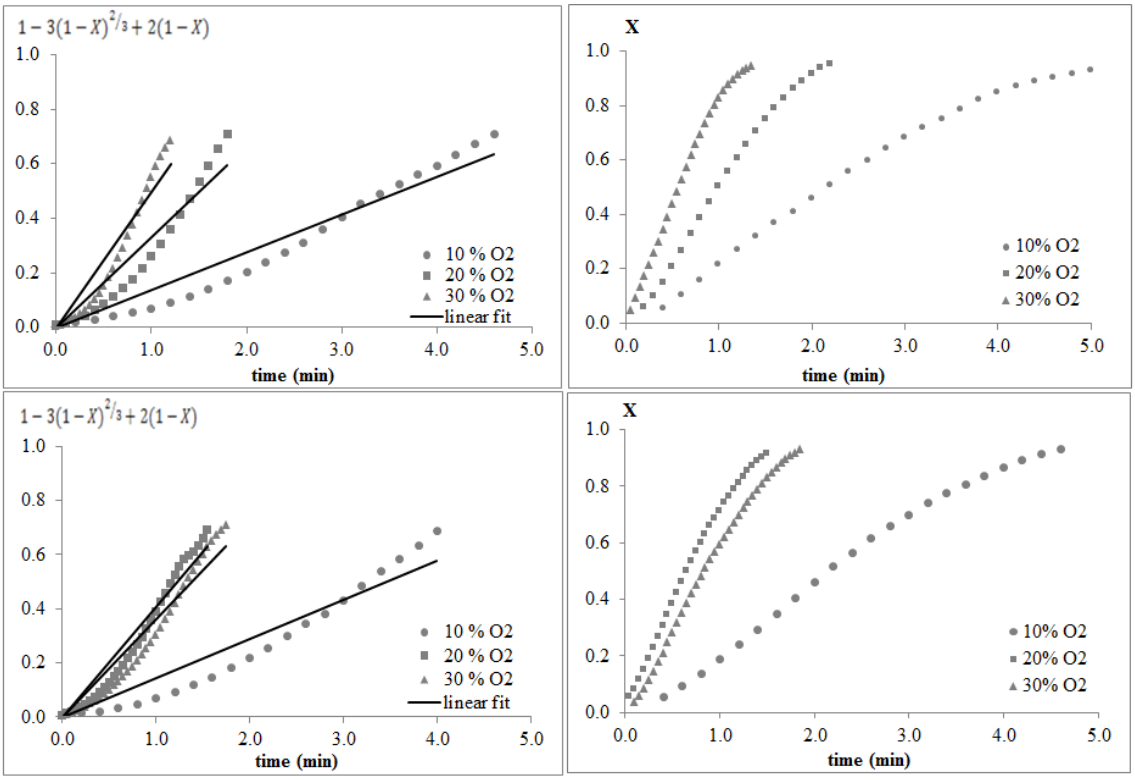

Figure 7: Curve-fit of the expression for the unreacted core model when diffusion of reagent gas in the ash layer controls the process and the curves of char conversion as a function of time for the temperatures 973 K, 1073 K, 1173 K and 1273 K.

In Figure 8, the fit of the experimental data collected at 973 K, 1073 K, 1173 K and 1273 K to the unreacted core model was calculated, considering step 3 of the reaction process to be the controlling step. In this case, a good fit of the experimental data to the model was achieved, indicating that the chemical reaction is indeed the controlling step of the reaction process.

At low concentrations of oxygen in the gaseous mixture, the reaction is slower and the determining character of the chemical kinetics becomes more evident.

When the chemical reaction controls the reaction process, the time τ for the full conversion of the particle is given by Equation (13):

$$\tau = \frac{\rho\, R}{k\, P_{O_2}} \tag{13}$$

where τ is the time for the full conversion (s), R is the radius of the *char* particles (m), ρ is the specific mass of the *char* sample (kg.m^{-3}), k is the superficial first-order reaction rate constant (kg.m^{-2}.s^{-1}.kPa^{-1}) and P_{O_2} is the partial pressure of oxygen (kPa).

If the rate of reaction ($-r_A$) is assumed to obey Equation (14),

$$\left(-r_A\right) = k\, P_{O_2}^{n} \tag{14}$$

where n is the order of the reaction and k is the superficial first-order reaction rate constant (kg.m^{-2}.s^{-1}.kPa^{-n}), then the rate of reaction ($-r_A$) can be calculated using Equation (15):

$$\left(-r_A\right) = \frac{R.\rho}{\tau} \tag{15}$$

where ($-r_A$) is the rate of reaction (kg.m^{-2}.s^{-1}), R is the radius of the *char* particles (= 3.63x10^{-4} m), ρ is the specific mass of the *char* sample (1960 kg.m^{-3}) and τ is the experimental value obtained from Figure 4 or 5.

By linearising Equation (14), the values of k and n can be determined. The pre-exponential factor, A (kmol.s^{-1}.m^{-2}), and the activation energy of the reaction, E_a (kJ.kmol^{-1}), can also be calculated via the Arrhenius equation. The Arrhenius equation is represented in Equation (16):

$$k = A\, exp\left(\frac{E_a}{\mathcal{R}T}\right) \tag{16}$$

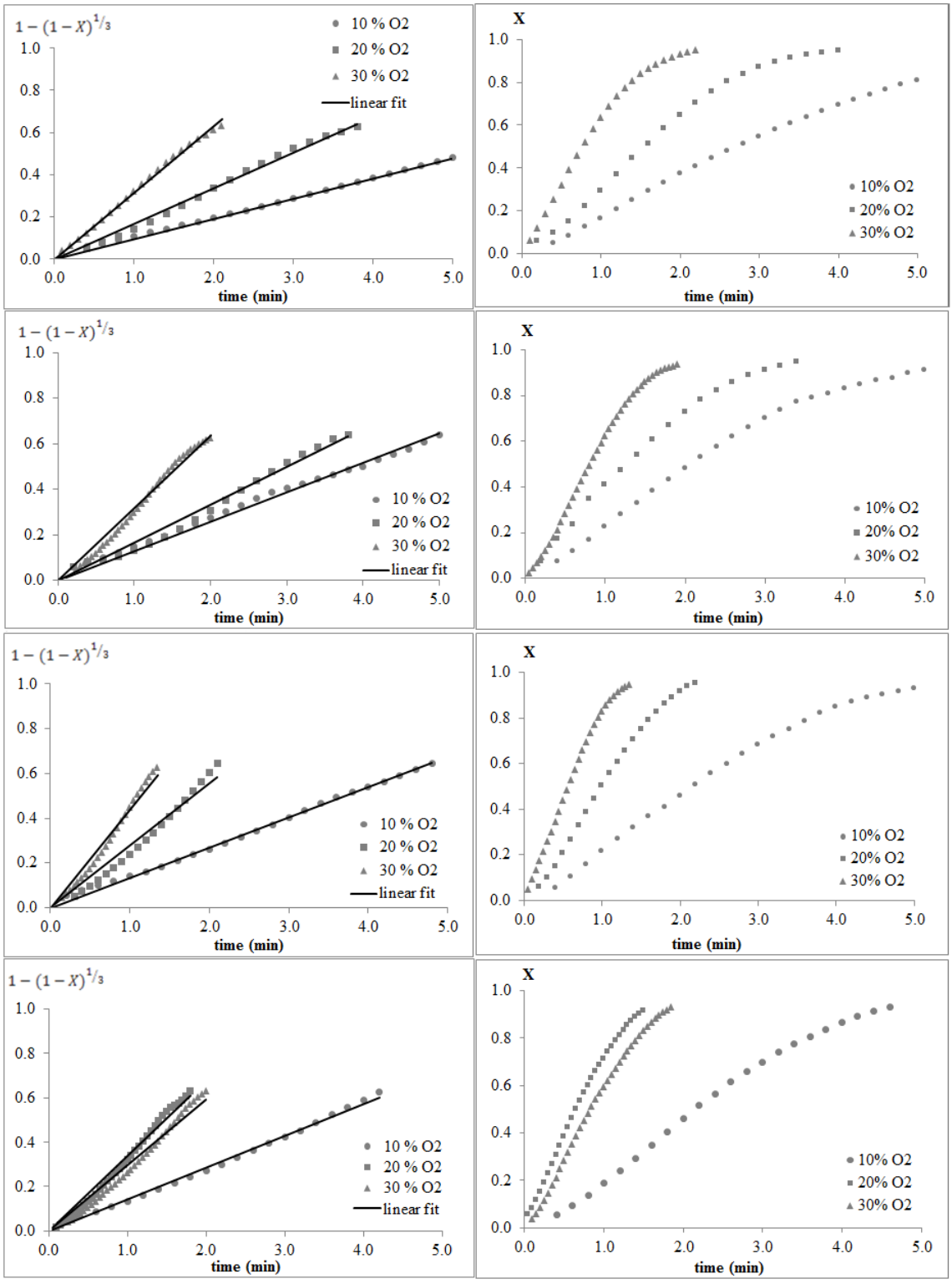

Figure 8: Curve-fit of the expression for the unreacted core model when the chemical reaction controls the process and the curves of *char* conversion as a function of time for the temperatures 973 K, 1073 K, 1173 K and 1273 K.

Figure 9 presents a graph of the linearised Arrhenius equation. Analysis of the behaviour of the results revels that a change occurs in the dominant reaction mechanism from chemically-controlled at low temperatures to diffusion-controlled at high temperatures.

Thus, for the unreacted core model, values of 56.7 kJ.kmol^{-1} for the energy of activation and 0.78 kmol.s^{-1}.m^{-2} for the pre-exponential factor were obtained for temperatures between 973 K and 1073 K. For temperatures between 1073 K and 1273 K, the activation energy was 23.4 kJ.kmol^{-1} and the pre-exponential factor was 0.56 kmol·s^{-1}·m^{-2}.

The order of reaction was 0.5 for 973 K and 0.7 for the other temperatures.

For the calculation of the kinetic parameters, the partial concentration of O_2 was considered as being proportional to the concentration of the reagent gas, a situation that occurs only at temperatures lower than 1073 K. For temperatures greater than 1073 K, it is also necessary to consider Boudouard's reaction because, in this case, reactions (17) and (18) occur simultaneously:

$$C + O_2 \rightarrow CO_2 \quad (17)$$

$$C + CO_2 \rightarrow 2CO \quad (18)$$

Figure 10 shows a sample of 30 mg of *char* on the platinum screen before being added to the thermobalance and the *char* obtained after oxy-fuel combustion. Because of the high ash content of the samples, the particles did not suffer size reduction after the oxy-fuel combustion process, which supports the hypothesis of the unreacted core model.

Continuous Reaction Model

The experimental data were not fit to the continuous reaction model.

The *char* particles used contained 59.7% ash scattered throughout their volume, making the consumption of carbon heterogeneous as the reaction proceeded to the interior of the particles. Therefore, the assumptions of the continuous reaction model were not satisfied in this case.

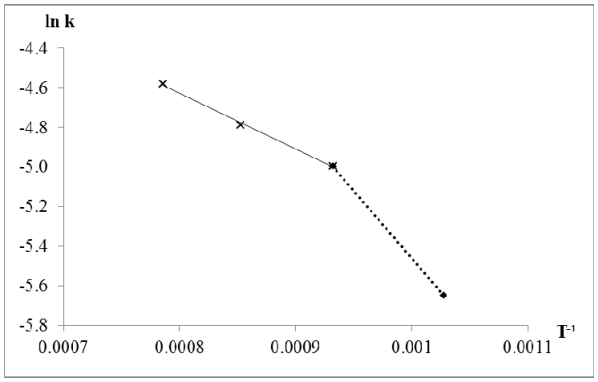

Figure 9: Effect of temperature on the reaction 2C + O_2 → 2CO.

Figure 10: *Char* before oxy-fuel combustion and ash after oxy-fuel combustion.

Langmuir-Hinshelwood Model

Considering that the rate of reaction ($-r_A$) can be expressed as the inverse of Equation (11), according to Equation (19), the specific rates k_1 and k_2 of reactions (9) and (10) can be evaluated through the determination of the angular and linear coefficients of the referred line:

$$\frac{1}{(-r_A)} = \frac{1}{k_2} + \frac{1}{P_{O_2}} \cdot \frac{1}{k_1} \tag{19}$$

Figure 11 shows the lines obtained at temperatures of 973 K, 1073 K, 1173 K and 1273 K using the Langmuir-Hinshelwood model to fit the experimental data of the oxy-fuel combustion of *char*.

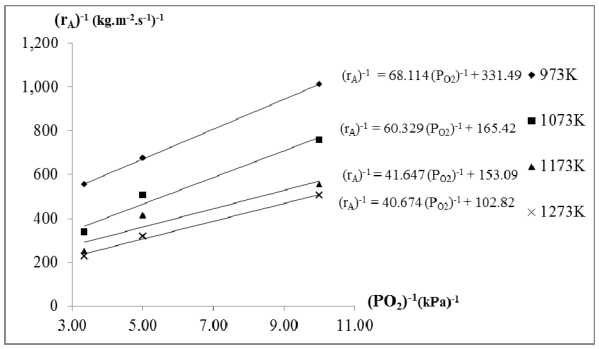

Figure 11: Graph obtained from the linearisation of Equation (17) for determination of the specific rates of reaction of each elementary step.

On the basis of the equations of the lines shown in Figure 10, the specific rates for each step of the elementary reactions (9) and (10) can be determined according to Equation (20) and (21):

$$k_1 = A_1 exp\left(\frac{-(E_a)_1}{\boldsymbol{R}T}\right) \tag{20}$$

$$k_2 = A_2 exp\left(\frac{-(E_a)_2}{\boldsymbol{R}T}\right) \tag{21}$$

Table 2 shows the results obtained for k_1 and k_2 for the temperatures 973 K, 1073 K, 1173 K and 1273 K.

As is evident from the results in Table 2, an increase in temperature causes the values of k_2 to increase more significantly than the values of k_1. This phenomenon indicates that increased temperature favours oxygen adsorption onto the active sites of the carbon over desorption of carbon monoxide from active sites; consequently, the reaction is zeroth-order (Hurt and Calo, 2001).

Table 2: Values of the rate constants for each elementary step of the equation.

Temperature (K)	k_1 (kmol.m^{-2}.s^{-1}).10^{+2}	k_2 (kmol.kPa.m^{-2}.s^{-1}).10^{+3}
973	1.468	3.017
1073	1.657	6.045
1173	2.401	6.532
1273	2.458	9.726

To determine the frequency and activation energy for each elementary step of the reaction, the Arrhenius Equation (20) and (21) were used in linearised form, as shown in Figure 12.

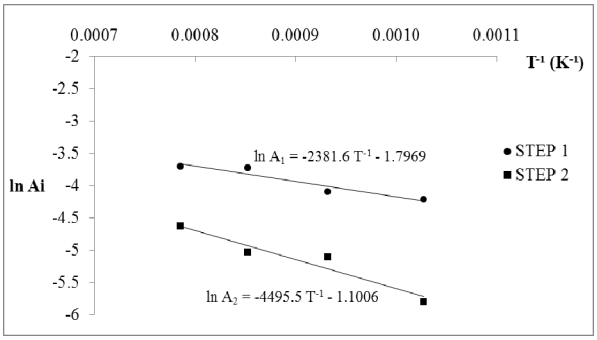

Figure 12: Chart for determining the activation energy and the frequency factor of the reactions (20) and (21).

The activation energy observed for step 1 of the reaction process was 19.8 kJ.kmol^{-1} (reaction 9), and that for step 2 was 37.3 kJ.kmol^{-1} (reaction 10). The pre-exponential factors for steps 1 and 2 of the reaction were 0.995 kmol.m^{-2}.s^{-1} and 2 kmol.kPa.m^{-2}.s^{-1} respectively.

CONCLUSIONS

A high-ash mineral coal from Mina do Leão II, southern Brazil, previously pyrolysed with N_2 at 1173 K, was used to study oxy-fuel kinetics (using mixtures of O_2/CO_2 in concentrations of 10, 20 and 30% O_2 in CO_2) at temperatures of 973, 1073, 1173 and 1273 K. The main conclusions of this study are as follows:

According to the unreacted core model, a change of reaction control within the range of investigated temperatures was observed. Below 1073 K, kinetic

control predominates in the reactions, with an activation energy of 23.4 kJ.kmol^{-1} and a pre-exponential factor of 0.093 kmol.s^{-1}.m^{-2}. Above this temperature, the control mechanism shifts and diffusion predominates, with an activation energy of 56.7 kJ.kmol^{-1} and a pre-exponential factor of 3.91 kmol.s^{-1}.m^{-2}. For the calculation of kinetic parameters, only the partial concentration of O_2 was considered as being proportional to the concentration of the reagent gas, a situation that occurs only at temperatures lower than 1073 K. For temperatures above 1073 K, the Boudouard reaction occurs simultaneously, which explains why the order of the reaction is 0.5 at 973 K and 0.7 at the other investigated temperatures.

Using the continuous reaction model did not yield a good fit to the experimental data because the model assumes a uniform consumption of carbon during the reaction, which does not occur experimentally because of the large amount of ash distributed throughout the *char* particles.

The activation energy determined for the C-O_2 reaction using the Langmuir-Hinshelwood model was 19.8 kJ.kmol^{-1} for the adsorption of oxygen atoms onto the active sites of the carbon and 37.3 kJ.kmol^{-1} for the desorption of carbon monoxide from the active sites. The reaction and desorption steps of the Langmuir-Hinshelwood model did not provide an exact value for the order of the reaction.

On the basis of the experimental results obtained in this study, we recommend that the unreacted core model be used to interpret data in the kinetic regime for the scaling and modelling of fluidised-bed oxy-fuel reactors using mineral coal with a high ash content.

NOMENCLATURE

A	pre-exponential factor	kmol.s^{-1}.m^{-2}
$\mathcal{D}_e$	coefficient of effective diffusivity	m².s^{-1}
E_a	activation energy	kJ.kmol^{-1}
k	superficial first-order reaction rate constant	kg.m^{-2}.s^{-1}.kPa^{-1}
k_g	coefficient of mass transfer between the fluid and solid	kg.m^{-2}.s^{-1}.kPa^{-1}
k_1	specific rate	kmol.m^{-2}.s^{-1}
k_2	specific rate	kmol.kPa.m^{-2}.s^{-1}
M_i	initial mass of the *char*	mg
M	instantaneous mass	mg
M_c	final mass after oxy-fuel combustion	mg
n	order of the reaction	
P_{O_2}	partial pressure of oxygen	kPa
R	radius of the *char* particles	m
$\boldsymbol{R}$	gas constant	8.314 kPa.m^3.kmol^{-1}.K^{-1}
$(-r_A)$	rate of reaction	kg.m^{-2}.s^{-1}
T	temperature	K
t	time	s

Greek Symbols

τ	time to complete the reaction,	s
ρ	specific mass of the *char* sample,	kg.m^{-3}

REFERENCES

BEM, Balanço Energético Nacional 2012, Ano Base 2011, Rio de Janeiro (2012). (In Portuguese).

Bachu, S., Bonijoly, D., Bradshaw, J., Burruss, R., Holloway, S., Christensen, N. P., Mathiassen, O. M., CO_2 storage capacity estimation: Methodology and gaps. International Journal of Greenhouse Control, 1, p. 430-443 (2007).

Barranco, R., Rojas, A., Barraza, J., Lester, E., A new char combustion kinetic model 1. Formulation. Fuel, 88, p. 2335-2339 (2009).

Buhre, B. J. P., Elliott, L. K., Sheng, C. D., Gupta, R. P., Wall, T. F., Oxy-fuel combustion technology for coal-fired power generation. Program in Energy and Combustion Science, 31, p. 283-307 (2005).

Cailly, B., Thiez, P., Egermann, P., Audibert, A., Vidal-Gilbert, S., Longaygue, X., Geological Storage of CO_2: A state-of-the-art of injection process and technologies. Oil & Gas Science and Technology, 60, p. 517-525 (2005).

Carotenuto, A., Silva, R. C., Rech, R. L., Marcílio, N. R., Schneider, P. S., Krautz, H. J., Preliminary investigation of the global kinetic parameters of low-rank coals under oxy-fuel conditions. 3th Brazilian Congress of Coal, Gramado (2011).

Carotenuto, A., Silva, R. C., Rech, R. L., Schneider, P. S., Marcilio, N. R., Krautz, H. J., Experimental analysis of low-rank coal combustion under air and oxy-fuel conditions. In: ENCIT 2012 14th Brazilian Congress of Thermal Sciences and Engineering, 2012, Rio de Janeiro, ENCIT, Rio de Janeiro: ABCM (2012).

EIA, Energy Information Administration – Emission of Greenhouse Gases in the United States 2009,

Washington (2011).

EIA, Energy Information Administration – International Energy Outlook (2012).

Gil, M. V., Riaza, J., Álvarez, L., Pevida, C., Pis, J. J., Rubiera, F., Oxy-fuel combustion kinetics and morphology of coal chars obtained in N_2 and CO_2 atmospheres in an entrained flow reactor. Applied Energy, 91, p. 67-74 (2011).

Hecht, E. S., Shaddix, C. R., Molina, A., Haynes, B. S., Effect of CO_2 gasification reaction on oxy-combustion of pulverized coal char. Proceeding of the Combustion Institute, 33, p. 1699-1706 (2011).

Hurt, R. H., Calo, J. M., Semi-global intrinsec kinetic for char combustion modeling. Combustion and Flame, 125, p. 1138-1149 (2001).

Irfan, M. F., Usman, M. R., Kusakabe, K., Coal gasification in CO_2 atmosphere and its kinetics since 1948: A brief review. Energy, 36, p. 12-40 (2011).

José, H. J., Zur Reaktivität von Koksen aus Santa Catarina-Steinkohle, Brasilien, bei der Vergasung mit Wasserdampf und Kohlendioxid. Thesis, RWTH Aachen, Germany (1989). (In German).

Khatami, R., Stivers, C., Joshi, K., Levendis, Y. A. and Sarofim, F. A., Combustion behavior of single particles from three different coal ranks and from suger cane bagasse in O_2/N_2 and O_2/CO_2 atmospheres. Combustion and Flame, 159, 1253-1271 (2012a).

Khatami, R., Stivers, C. and Levendis, Y. A., Ignition characteristics of single coal particles from three different ranks in O_2/N_2 and O_2/CO_2 atmospheres. Combustion and Flame, 159, p. 3554-3568 (2012b).

Kazanc, F., Khatami, R., Manoel-Crnkovic, P., Levendis, Y. A., Emissions of NOx and SO_2 from coals of various ranks, bagasse and coal-bagasse blends burning in O_2/N_2 and O_2/CO_2 Environments. Energy and Fuels, 25(7), 2850-2861 (2011).

Levenspiel, O., Chemical Reaction Engineering. 3th Ed., New York, John Wiley & Sons (1976).

Li, Q., Zhao, C., Chen, X., Wu, W., Li, Y., Comparison of pulverized coal combustion in air and in O_2/CO_2 mixtures by thermo-gravimetric analysis. Journal of Analytical and Applied Pyrolysis, 85, p. 521-528 (2009).

Liu, H., Zailani, R., Gibbs, B. M., Comparisons of pulverized coal combustion in air and in mixtures of O_2/CO_2. Fuel, 84, p. 833-840 (2005).

Middleton, D., Mcculloch, M., Miller, P., Normand, E., Cassels, G., Bullock, A., Jacobina, E., Trial CO_2 measurement and capture system incorporating hybrid inorganic membranes for flue gas cleaning. Journal of Membrane Technology, 2011, p. 7 -10 (2011).

Qanbari, F., Pooladi-Darvish, M., Tabatabaie, S. H., Gerami, S., Storage of CO_2 as hydrate beneath the ocean floor. Energy Procedia, 4, p. 3997-4004 (2011).

Schmal, M., Monteiro, J. L. F., Castellan, J. L., Kinetics of coal gasification. Ind. Eng. Chem. Process Des. Dev., 21, p 256-266 (1982).

Soares, P. S. M., Santos, M. D. C., Possa, M. V., Carvão brasileiro: Tecnologia e meio ambiente. Sci. and Technol., (2008). (In Portuguese).

Stanger, R., Wall. T., Sulphur impacts during pulverized coal combustion in oxy-fuel technology for carbon capture and storage. Progress in Energy and Combustion Science, 37, p. 69-88 (2011).

Toftegaard, M. B., Brix, J., Jensen, P. A., Glarborg, P., Jensen, A. D., Oxy-fuel combustion of solid fuel. Progress in Energy and Combustion Science, 36, p. 581-625 (2010).

Wall, T., Liu, Y., Spero, C., Elliot, L., Khare, S., Rathnam, R., Zeenathal, F., Moghtaderi, B., Buhre, B., Sheng, C., Gupta, R., Yamada, T., Makino, K., Yu, J., An overview on oxy-fuel coal combustion – State of the art research and technology development. Chemical Engineering Research and Design, 87, p. 1003-1016 (2009).

WCI, World Coal Institute. The Coal Resource. A Comprehensive Overview of Coal, London, UK (2005).